

**Role of Magnetic Resonance Imaging in Characterization of Posterior Cranial Fossa Masses****Ghada Mohamed Abdelrazek<sup>a</sup>, Eslam Sayed Elkhateeb<sup>b</sup>, Rania Mohamed Ali Mahmoud<sup>a\*</sup>, AbdAlRaheem Husein Ali<sup>a</sup>**<sup>a</sup>Diagnostic and Interventional Radiology Department , Faculty of Medicine, South Valley University, Qena, Egypt.<sup>b</sup>Neurosurgery Department , Faculty of Medicine, South Valley University, Qena, Egypt.**Abstract**

**Background:** Posterior fossa tumors have a wide range of differential diagnosis. Accurate radiological differentiation by magnetic resonance imaging which is the imaging technique of choice in assessing the site and the extent of the tumor is important for determining the correct treatment plan.

**Objectives:** To evaluate the value of MRI in localization, extension, characterization, differentiation of posterior fossa masses.

**Patients and methods:** This was cross sectional study done at interventional and diagnostic radiology department at Qena university hospital on 50 patients with posterior cranial fossa masses. All studied cases underwent a full history taking and MRI scans of the brain in a supine position. MRI results were compared with histopathological assessment in undetermined cases.

**Results:** 26 (52%) cases were under 16 years old. MRI revealed that 16 (32%) diagnosed cases as pilocytic astrocytoma, 7 (14%) as glioma, 6 (12%) each of ependymoma, acoustic neuroma, metastasis and medulloblastoma, two (4%) as meningioma and one (2%) as arachnoid cyst. On T1WI, 92% were hypointense on T1WI. On T2WI, 70% were hyperintense, whereas 16% were heterogeneous. On FLAIR, most of tumors were hyperintense (64%). On post-contrast images, the majority of the tumors showed both heterogenous post-contrast enhancement (34%) and enhanced mural nodule (30%).

**Conclusion:** It was found that the MRI is a golden tool in characterization of these masses as it demonstrated the extent of the tumor and the amount to which the surrounding tissues were involved, thus aiding in the management of tumors. In most cases, the histopathologic diagnosis and the MR diagnostic imaging are correlated.

**Keywords:** Magnetic resonance imaging; Posterior fossa; Masses.

DOI: 10.21608/SVUIJM.2023.239832.1711

\*Correspondence: [Raniamali483@gmail.com](mailto:Raniamali483@gmail.com)

Received: 20 September, 2023.

Revised: 17 October, 2023.

Accepted: 10 November, 2023.

Published: 8 May, 2025

Cite this article as Ghada Mohamed Abdelrazek, Eslam Sayed Elkhateeb, Rania Mohamed Ali Mahmoud, AbdAlRaheem Husein Ali. (2025). Role of Magnetic Resonance Imaging in Characterization of Posterior Cranial Fossa Masses. *SVU-International Journal of Medical Sciences*. Vol.8, Issue 1, pp: 1172-1182.

Copyright: © Abdelrazek et al (2025) Immediate open access to its content on the principle that making research freely available to the public supports a greater global exchange of knowledge. Users have the right to Read, download, copy, distribute, print or share link to the full texts under a [Creative Commons BY-NC-SA 4.0 International License](https://creativecommons.org/licenses/by-nc-sa/4.0/)

## Introduction

The posterior fossa tumors have been regarded as critical brain lesions. They are very common in children compared to the adults (O'Brien et al, 2001), having a wide range of differential diagnosis. In adults, cerebellar metastases are the most common posterior fossa tumor, whereas hemangioblastoma is the most common primary posterior fossa tumor (Grossman et al, 2016). In children, pilocytic astrocytoma and medulloblastoma are the most common posterior cranial fossa tumors. (Kerleroux et al, 2020).

Accurate radiological differentiation of brain masses is important to determine the best treatment plan. MRI is the imaging modality of choice in evaluating lesions arising in the posterior fossa, it is the best means of localizing lesions and determining the extent of disease. Conventional MR imaging has a success rate of 30-90% in diagnosis. However, advanced MRI sequences such as diffusion-weighted imaging (DWI), MR perfusion, and magnetic resonance spectroscopy (MRS) can give information regarding the tissue constituents within a mass, such as the existence of cellularity, necrosis, and bleeding. (Baghdady et al, 2016).

The aim of this study was to determine the additional value of magnetic resonance imaging (MRI) in the characterization, localization, extension, and distinction of various posterior fossa masses.

### Patients and methods:

This was cross sectional study done at interventional and diagnostic radiology department at Qena university hospital, Egypt. Sample Size: 50 patients with posterior cranial fossa masses.

**Inclusion criteria:** Patients with posterior cranial fossa mass lesions benign and malignant with no age limitations.

**Exclusion criteria:** posterior fossa strokes, posterior fossa inflammatory lesions, posterior cranial fossa autoimmune diseases, post-traumatic Posterior fossa lesions.

**Methods:** All studied cases underwent:

- Good history taking (personal history, family history and surgery history).

- Investigations: an MRI scan of the brain by Philips achievea 1.5T MRI sytem. patient in a supine position, the following sequences will be obtained using 4-5 mm slice thickness (Morani et al., 2011):

- T1 weighted in different planes
  - Purpose: anatomical overview including the soft tissues.
- T2 weighted in different planes
  - Purpose: assessment of the ventricular system, basal cisterns, subdural spaces and presence of edema.
- FLAIR in axial plan
  - Purpose: evaluation of the involvement of the white matter and related vasogenic edema.
- Diffusion-weighted imaging (DWI) in axial
  - Purpose: evaluation of the cellularity of the tumor.
- Post-contrast sequences in different planes using Gadolinium-based contrast agent (GBCA) for CNS.
  - GBCA administered dose was 0.2mmol/kg body weight.
- MRI of the brain was performed and reported by a qualified radiologist.
- MRI results will be compared with histopathological assessment in undetermined cases.

### Ethical considerations:

Research was accepted by Faculty's Ethics Committee, South Valley University (Approval code: SVU-MED-RAD028-1-22-2-329). All study participants will provide informed

written consent. This work was performed in accordance with the World Medical Association's Code of Ethics for human researches (Declaration of Helsinki).

### Statistical analysis

The collected data were statistically analyzed using SPSS program (Statistical Package for Social Sciences) software version 26.0. Descriptive statistics were done for numerical parametric data as Mean $\pm$ SD and categorical data as number and percentage. The level of significance was taken at P value <0.05 is significant, otherwise is non-significant. Distance matrix based on Manhattan coefficient was calculated using the computer software program "Community Analysis Package" (CAP) 4.0. The CAP software was also used

for cluster analysis to measure the relationships between the tumors based on Manhattan coefficient estimates using ward tree building methods. The cluster analysis was also performed using the NT-SYS-pc program version 2.0 to construct a dendrogram tree by UPGMA (unweighted pair group method with arithmetic averages).

### Results

#### Age distribution

(Table.1) shows demographic features of the studied patients. The ages of studied cases were in the range between 7 to 77 years with the average mean age of  $26 \pm 19.9$  years.

There are 26 (52%) children (16 years or less) and 24 (48%) adults (more than 16 years). However, there is a male predominance (36%) among children (male: female=2.25:1).

**Table 1. Age distribution**

| Variables                           | Age Distribution |      |
|-------------------------------------|------------------|------|
|                                     | Total            | %    |
| $\leq 16$ years                     | 26               | 52%  |
| $> 16$ years                        | 24               | 48%  |
| <b>Total</b>                        | 50               | 100% |
| <b>Age (Mean<math>\pm</math>SD)</b> | $26 \pm 19.9$    |      |

#### Radiological findings

MR study revealed 16 (32%) diagnosed cases as pilocytic astrocytoma (PA), 7 (14%) cases as glioma (G), 6 (12%) cases each of ependymoma (Ep), acoustic neuroma

(AN), metastasis (Met) and medulloblastoma (Med) as well as two (4%) cases as meningioma (Men) in addition to one (2%) case as arachnoid cyst (AC) as shown in (Table.2).

**Table 2. Distribution of studied patients regarding MR diagnosis**

| Parameters          |                       | Studied patients |     |
|---------------------|-----------------------|------------------|-----|
|                     |                       | (n= 50)          |     |
|                     |                       | N                | %   |
| <b>MR diagnosis</b> | Pilocytic astrocytoma | 16               | 32% |
|                     | Glioma                | 7                | 14% |
|                     | Ependymoma            | 6                | 12% |
|                     | Acoustic neuroma      | 6                | 12% |
|                     | Metastasis            | 6                | 12% |
|                     | Medulloblastoma       | 6                | 12% |
|                     | Meningioma            | 2                | 4%  |
|                     | Arachnoid cyst        | 1                | 2%  |

n: number, %: percentage.

**Tumor pattern on conventional (t1-t2-flair) and post contrast MRI images**

Presented data in (Table.3) show Tumor pattern on conventional and post contrast MRI. On T1WI, most of the cases displayed a hypointense signal (92%) while 7% displayed isointense signal. On T2WI, most of the cases were primarily hyperintense, whereas 16% displayed a heterogeneous signal. Moreover, 14.0% of the cases were isointense. On FLAIR that most of the tumors were hyperintense (64%),16% showed

heterogenous signals. Moreover, 14% were isointense. However, 6% showed hypointense. On post-contrast images, the majority of the tumors showed both heterogenous post-contrast enhancement (Hetero., 34%) and enhanced mural nodule (Enh. M.N., 30%) with no significant differences between them followed by homogenous post-contrast enhancement (Homo., 28%). However, there was no appreciable enhancement in 6%. The least common pattern was peripheral enhancement (2%). (Figs.1, 2 & 3).

**Table 3. Tumor pattern on conventional (T1-T2-FLAIR ) and post contrast MRI images**

| Variab les    |                       | Pilocytic astrocytoma | Ependymoma | Glioma | Acoustic neuroma | mets | Arachnoid cyst | Medullo blastoma | Meningiom a | Total (%) |
|---------------|-----------------------|-----------------------|------------|--------|------------------|------|----------------|------------------|-------------|-----------|
|               | <i>hypointense</i>    | 16                    | 5          | 7      | 6                | 6    | 1              | 5                | 0           | 46(92%)   |
| <b>T1</b>     | <i>Isointense</i>     | 0                     | 1          | 0      | 0                | 0    | 0              | 1                | 2           | 4(8%)     |
|               | <i>Hyperintens e</i>  | 15                    | 6          | 6      | 0                | 6    | 1              | 1                | 0           | 35(70%)   |
| <b>T2</b>     | <i>heterogenou s</i>  | 1                     | 0          | 1      | 6                | 0    | 0              | 0                | 0           | 8(16%)    |
|               | <i>Isointense</i>     | 0                     | 0          | 0      | 0                | 0    | 0              | 5                | 2           | 7(14%)    |
|               | <i>hypointense</i>    | 2                     | 0          | 0      | 0                | 0    | 1              | 0                | 0           | 3(6%)     |
| <b>FLAI R</b> | <i>hyperintens e</i>  | 13                    | 6          | 6      | 0                | 6    | 0              | 1                | 0           | 32(64%)   |
|               | <i>hetrogenous</i>    | 1                     | 0          | 1      | 6                | 0    | 0              | 0                | 0           | 8(16%)    |
|               | <i>Isointense</i>     | 0                     | 0          | 0      | 0                | 0    | 0              | 5                | 2           | 7(14%)    |
|               | <i>E.M.N</i>          | 15                    | 0          | 0      | 0                | 0    | 0              | 0                | 0           | 15(30%)   |
| <b>Post</b>   | <i>Heteogenou s</i>   | 1                     | 5          | 6      | 5                | 0    | 0              | 0                | 0           | 17(34%)   |
| <b>GAD</b>    | <i>Homogenou s</i>    | 0                     | 1          | 0      | 0                | 5    | 0              | 6                | 2           | 14(28%)   |
|               | <i>Periph.Enh anc</i> | 0                     | 0          | 0      | 0                | 1    | 0              | 0                | 0           | 1(2%)     |
|               | <i>No.Enhanc</i>      | 0                     | 0          | 1      | 1                | 0    | 1              | 0                | 0           | 3(6%)     |

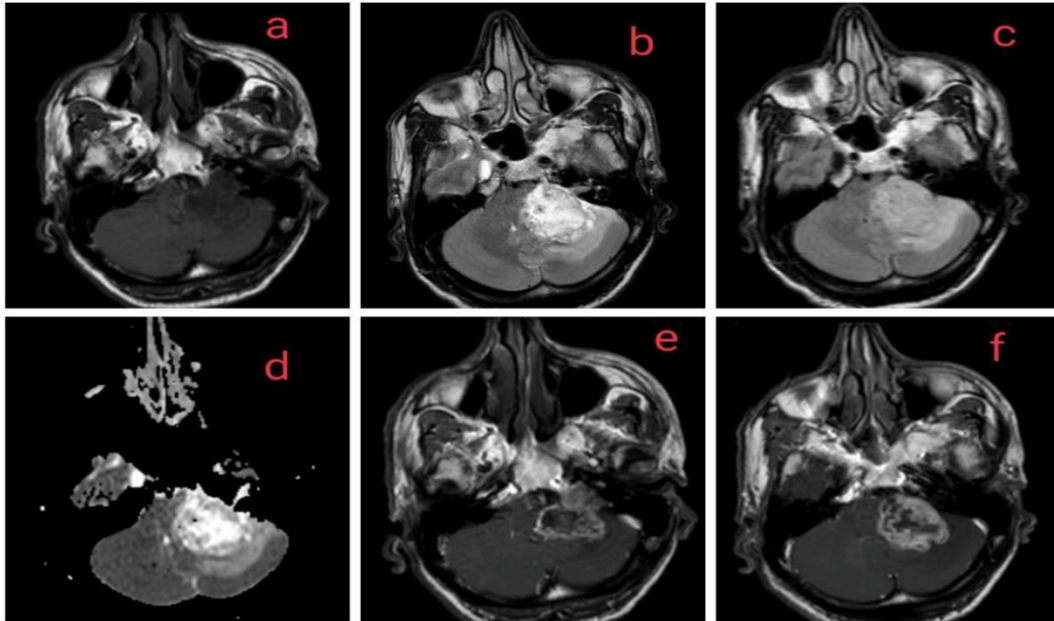


**Fig.1.** A 61 year old male patient has progressive right- sided hearing loss for 3 years .MRI: ( a) Axial T1WI: Show posterior fossa hypointense lesion.(b&c) Axial T2WI and FLAIR image: show extra-axial hyperintense left CPA lesion(d) ADC: The lesion show facilitated diffusion.(e&f) Axial T1 weighted Post contrast images: the lesion show heterogenous enhancement. vestibular shwannoma is histopathologically proved.

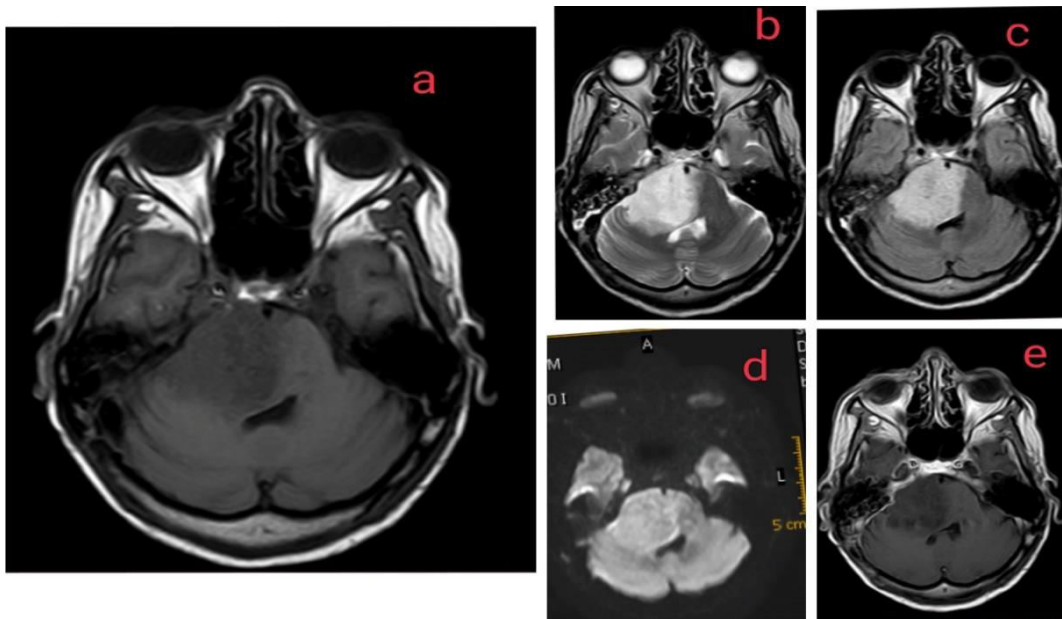


**Fig.2.** Female patient 42 years old presented by headache, generalized weakness, 5<sup>th</sup> and 7<sup>th</sup> cranial nerves palsy for two years duration. MRI shows: (a) Axial T1WI: shows diffuse hypointense pontine lesion.(b&c) Axial T2WI and Axial FLAIR Image: the lesion appears hyperintense (d) DWI: It shows facilitated diffusion.(e) Axial T1 weighted post contrast image: there is no post contrast enhancement. cellular ependymoma is histopathologically proved.

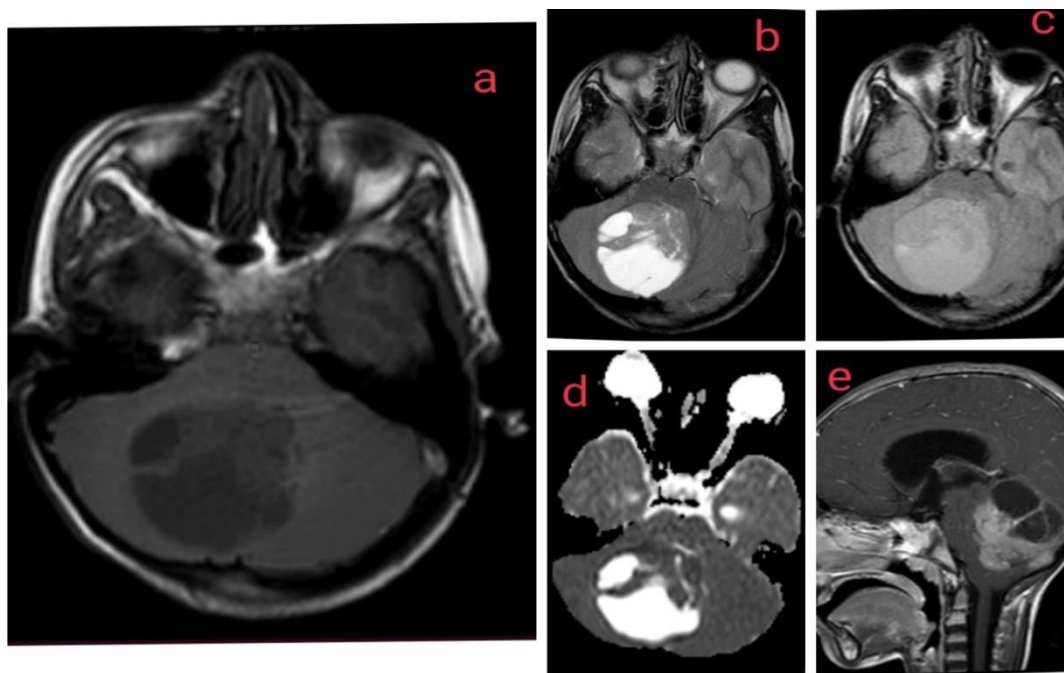


**Fig.3. Female patient 9 years old presented with headache, nausea, vomiting and disturbed conscious level.** MRI shows: (a) Axial T1WI: Mixed intensity lesion in right cerebellar hemisphere.(b&c) Axial T2WI and FLAIR images: show well defined hyperintense cystic lesion with mural nodule (d) ADC image: It shows facilitated diffusion with restricted mural nodule. (e)T1 Weighted post-contrast sagittal Image: It shows enhanced mural nodule. Pilocytic astrocytoma is histopathologically proved *Correlation of MR diagnosis with histopathologic diagnosis* with histopathologic diagnosis that was histopathological confirmation was

It can be seen from the data in (Table.4) the correlation of MR diagnosis established in 43 out of 50 cases.

**Table 4. Correlation of MR diagnosis with histopathologic diagnosis**

| MR Diagnosis                 | HP       |          | Total | %    |
|------------------------------|----------|----------|-------|------|
|                              | Positive | Negative |       |      |
| <b>Pilocytic astrocytoma</b> | 14       | 2        | 16    | 37%  |
| <b>Ependymoma</b>            | 5        | 1        | 6     | 14%  |
| <b>Glioma</b>                | 5        | 2        | 7     | 16%  |
| <b>Acoustic neuroma</b>      | 5        | 1        | 6     | 14%  |
| <b>Medulloblastoma</b>       | 5        | 1        | 6     | 14%  |
| <b>Meningioma</b>            | 2        | 0        | 2     | 5%   |
| <b>Total</b>                 | 36       | 7        | 43    | 100% |
| <b>%</b>                     | 84%      | 16%      | 100%  |      |

Six cases of metastasis and one case of the arachnoid cyst were among the seven patients in whom the histopathologic evaluation was not obtained. The primary tumor (1ry) was known in metastases. The arachnoid cyst had the typical MR signs (adequate MRI data), however, the dangerous biopsy in this area was skipped because of the higher

incidence of complications. However, MRI correctly diagnosed 36 out of 43 patients with a positive predictive value of 84%.

*Sensitivity (S), specificity (Sp), both positive (PPV) and negative (NPV) predictive values as well as accuracy of the MRI in the different types of studied tumors*

The sensitivity (S) of MR to diagnose glioma, acoustic neuroma, meningioma, pilocytic astrocytoma, medulloblastoma, ependymoma and hemangioblastoma were 100%, 100%, 100%, 92.86%, 83.33%, 71.43% and 50%, in descending order. However, specificity values showed 100% for meningioma and hemangioblastoma, > 97% for each ependymoma, acoustic neuroma, and medulloblastoma as well as 94.74% and 93.10% for glioma and pilocytic astrocytoma, respectively. Moreover, positive predictive values (PPV) were 100 % (Meningioma and Hemangioblastoma), 86.67 % (Pilocytic astrocytoma), 83.33 % (each of medulloblastoma and

ependymoma), acoustic neuroma (80%) and 71.43 % (Glioma), in descending order whereas, negative predictive value (NPV) showed 100 % for each of glioma, acoustic neuroma and meningioma followed by medulloblastoma (97.30%), pilocytic astrocytoma (96.43 %), hemangioblastoma (95.12%) and ependymoma (94.59 %). Therefore, the accuracy of MR to diagnose meningioma, acoustic neuroma, medulloblastoma, glioma, hemangioblastoma, ependymoma and pilocytic astrocytoma were 100 %, 97.67 %, 95.35 %, 95.35 %, 95.35%, 93.02 % and 93.02 %, respectively, (Table.5).

**Table 5. Sensitivity, specificity, PPV, NPV as well as accuracy of MRI**

| Item                         | S       | Sp      | PPV     | NPV     | Accuracy |
|------------------------------|---------|---------|---------|---------|----------|
| <b>Pilocytic astrocytoma</b> | 92.86%  | 93.10%  | 86.67%  | 96.43%  | 93.02%   |
| <b>Ependymoma</b>            | 71.43%  | 97.22%  | 83.33%  | 94.59%  | 93.02%   |
| <b>Glioma</b>                | 100.00% | 94.74%  | 71.43%  | 100.00% | 95.35%   |
| <b>Acoustic neuroma</b>      | 100.00% | 97.44%  | 80.00%  | 100.00% | 97.67%   |
| <b>Medulloblastoma</b>       | 83.33%  | 97.30%  | 83.33%  | 97.30%  | 95.35%   |
| <b>Meningioma</b>            | 100.00% | 100.00% | 100.00% | 100.00% | 100.00%  |
| <b>Hemangioblastoma</b>      | 50.00%  | 100.00% | 100.00% | 95.12%  | 95.35%   |

### Discussion

MRI of 50 patients who presented with posterior fossa tumor were studied prospectively in Qena Medical College Hospital.

The age of the patients in our study range from seven to seventy-seven years. The majority of the patients were children (52%). Pilocytic astrocytoma was the most common tumor among children. Among adults (48%), the most common tumor was acoustic neuroma and metastasis. **Mohammed (2021)** studied 46 patients who presented with posterior fossa tumors and discovered similar incidences.

MRI features of variable lesions were evaluated including their location, morphology and signal characteristics on multiple sequences

T1W, T2W, FLAIR, and post-contrast images.

There were 16 cases of pilocytic astrocytoma in our study. The most of the patients were male. Most 16 cases showed hypointense signal on T1WI and hyperintense signal on T2WI/FLAIR imaging and intense enhancement was seen.

**Bose et al., 2023**, found that Pilocytic astrocytoma was the most common tumor in among the included 30 patients. In the study of **Di-Napoli et al., 2021**, MRI was used to stay the characters of Pilocytic astrocytoma. They found that the target appearance with a T1-hypointense and was actively homogenous and slightly hyperintense signal T2-weighted images. Also, the tumor appeared as an enhanced on Coronal T2-FLAIR.

**Koeller and Rushing (2004)** described astrocytoma as a well circumscribed cystic rounded lesions with a solid nodule. The cystic element showed hypointense signal on T1WI, hyperintense signal on T2WI and hypointense signal on FLAIR. The solid nodule was isointense to grey matter on T1WI, hyperintense to grey matter but hypointense to CSF on T2WI and hyperintense to grey matter on FLAIR. It showed Intense enhancement on post contrast images.

**Qiu and Zhang (2003)** described MRI findings of 13 cases of intracranial ependymomas. The T1W images displayed isointense or hypointense signals and T2W/FLAIR images showed inhomogeneous hyperintense signals and the contrast-enhanced images presented inhomogeneous enhancement. There were 6 cases of ependymoma in the present study with similar features.

**Li et al.(2023)** conducted his study on 114 cases with suspected Ependymoma, On MR images, Ependymoma usually has a mixed cystic and solid appearance, the tumor parenchyma showed slightly iso-to-low intensity on T1WI, slightly moderate-to-high intensity on T2WI, and moderate-to-high intensity on T2-FLAIR, with obvious cystic degeneration and necrosis.

In the current study group, there were 7 cases of glioma. 2 out of the 7 patients were children and MRI characteristics were similar to those reported by **Zimmerman (1996)**.

According to **Menze et al.(2021)**, Glioma appeared as visible as hypointense areas in T1w hyper-intense areas in T2w and FLAIR images, the tumor core visible heterogenous signals in T2w MRI and the active tumor visible from intensity enhancements in post-Gd T1w scans.

Acoustic neuroma, it also called vestibular schwannoma, is a slow-growing, benign tumor that develops on the eighth cranial nerve. All six cases of the current study were centered on the internal auditory meatus (**Mulkens et al., 1993**). All cases displayed low signal on T1WI,

mixed signal on T2WI / FLAIR, and intense but heterogeneous enhancement. These results are similar to those of **Mohammed (2021)**.

Brain metastases occur when cancer cells spread from their original site to the brain. Any cancer can spread to the brain, but the types most likely to cause brain metastases are lung, breast, colon, kidney and melanoma. The lesions were multiple. the 5 Metastasis cases, i.e., 3 female (30-53 years) and 2 males (49-51 years) showed homogenous post-contrast enhancement (Homo., 10%) and only one female case (38 years) exhibited peripheral enhancement (peripheral, 2%). These findings were in agreement to those established by **Mohammed (2021)**.

Arachnoid cysts are benign and asymptomatic lesions arising in the central nervous system. In the current study arachnoid cysts were identified in one patient (2%). On all sequences, the intensity was identical to cerebrospinal fluid (CSF). as they are filled with CSF. These findings were consistent with the findings of **Dutt et al. (2002)**.

**Li et al.(2020)**, found that among 6978 with suspected tumor masses who underwent MRI, only 36 patients had arachnoid cyst. Furthermore, **Di-Studio et al.(2021)**, found that on MRI, arachnoid cyst was presented as a hypointense lesion on T and FLAIR.

There were six children presented with medulloblastoma, occupying the fourth ventricle, On T2W/FLAIR imaging, 5 cases were isointense and one patient on T1WI. It showed homogeneous post contrast enhancement. These findings are like those reported by **Rodallec et al. (2004)**.

The current study included two female cases of meningioma. The tumor was isointense on T1WI and

T2W/FLAIR imaging. **Maiuri et al. (1999)** observed similar findings. The case demonstrated homogenous enhancement. Our findings were consistent with those of **Mohammed (2021)**. They stated that meningiomas are more common in women.

Histopathological confirmation was established in 43 of 50 cases. Six cases of metastasis and one case of the arachnoid cyst were among the seven patients who did not have histopathologic examinations. The primary tumor (1ry) was known in metastases. The arachnoid cyst had the typical MR signs (adequate MRI data), however, the dangerous biopsy in this area was skipped because of the higher incidence of complications. However, MRI correctly diagnosed 36 of 43 patients, with a positive predictive value of 97.2%.

MRI was shown to be 97.4 to 100% highly sensitive and specific in identifying most posterior fossa tumors, i.e., meningioma and acoustic neuroma. In cases of brainstem glioma, MRI was 100% sensitive (S) and 100% negative predictive value (NPV) in cases of brainstem glioma. The specificity (Sp) was 94.74%, while the positive predictive value (PPV) was just 71.4%, bringing the accuracy down to 95.35%. In cases of Medulloblastoma, MRI was 83.3% sensitive and 97.3% negative predictive value. MR was also discovered to have a high specificity of 97.3%. The positive predictive value, on the other hand, was just 83.3%. Overall, MR had a 95.2% accuracy rate in diagnosing medulloblastoma. MRI was 71.4% sensitive and had a negative predictive value of 94.4% in cases of ependymoma. MR was also discovered to have a high specificity of 97.2%. The positive predictive value, on the other hand, was just 83.3%. Overall, MR had a 93.02% accuracy rate in diagnosing ependymoma.

Furthermore, in cases of hemangioblastoma, MRI was 50% sensitive and had a negative predictive value of 95.12%. MR was also found to have a high specificity and a 100% positive predictive value. Overall, MR was 95.35% accurate in diagnosing hemangioblastoma.

### Conclusion

It was found that the MRI is a golden tool in characterization of these masses as it revealed the exact extent of the tumor as well as the involvement of surrounding tissues, assisting in tumor management. In most cases, the histopathologic diagnosis and the MR diagnostic imaging are correlated.

**Conflicts of Interest:** authors declare that they have no conflicts of interest with respect to publication of this paper.

### References

- **Abdelhameed E, Morsy AA .(2021)**. Surgical outcome of primary intradural spinal arachnoid cysts: a series of 10 cases. The Egyptian Journal of Neurology, Psychiatry and Neurosurgery, 57(1): 1-6.
- **Baghdady AI, Maaly MA, El-wakeel AM, Mousa WA .(2016)**. The role of diffusion-weighted MRI in the evaluation and differentiation of space-occupying brain lesions. Menoufia Medical Journal, 29(2): 303.
- **Bose A, Prasad U, Kumar A, Kumari M, Suman SK, Sinha DK, et al. (2023)**. Characterizing Various Posterior Fossa Tumors in Children and Adults With Diffusion-Weighted Imaging and Spectroscopy. Cureus, 15(5): 2-27.
- **Di-Napoli A, Spina P, Cianfoni A, Mazzucchelli L, and Pravata E. (2021)**. Magnetic resonance imaging of pilocytic astrocytomas in adults with histopathologic correlation: a report of six consecutive cases. Journal of

- Integrative Neuroscience, 20(4): 1039-1046.
- **Di-Stadio A, Dipietro L, Messineo D, Ralli M, Ricci G, Greco A, et al. (2021).** Arachnoid Cysts of the Internal Auditory Canal: Multiplanar Magnetic Resonance Imaging With Audio-Vestibular Correlates. *The Laryngoscope*, 131(10): 2323-2331.
  - **Dutt SN, Mirza S, Chavda SV, Irving RM. (2002).** Radiologic differentiation of intracranial epidermoids from arachnoid cysts. *Otology & neurotology*, 23(1): 84-92.
  - **Grossman R, Ram Z. (2016).** Posterior fossa intra-axial tumors in adults. *World neurosurgery*, 88(1): 140-145.
  - **Kerleroux B, Cottier JP, Janot K, Listrat A, Sirinelli D, Morel B et al. (2020).** Posterior fossa tumors in children: radiological tips & tricks in the age of genomic tumor classification and advance MR technology. *Journal of Neuroradiology*, 47(1): 46-53.
  - **Koeller KK and Rushing EJ. (2004).** From the archives of the AFIP: pilocytic astrocytoma: radiologic-pathologic correlation. *Radiographics*, 24(6), 1693-1708.
  - **Li L, Begbie F, Grimmond N, and Kontorinis G. (2020).** Arachnoid cysts on magnetic resonance imaging: just an incidental finding?. *The Journal of Laryngology & Otology*, 134(5): 424-430.
  - **Li L, Fu Y, Zhang Y, Mao Y, Huang D, Yi X, et al. (2023).** Magnetic resonance imaging findings of intracranial extraventricular ependymoma: A retrospective multi-center cohort study of 114 cases. *Cancer Medicine*, 12(15), 16195-16206.
  - **Maiuri F, Iaconetta G, De Divitiis O, Cirillo S, Di Salle F, De Caro ML et al. (1999).** Intracranial meningiomas: correlations between MR imaging and histology. *European journal of radiology*, 31(1): 69-75.
  - **Menze B, Isensee F, Wiest R, Wiestler B, Maier-Hein K, Reyes M, et al. (2021).** Analyzing magnetic resonance imaging data from glioma patients using deep learning. *Computerized medical imaging and graphics*, 88, 101828.
  - **Mohammed F. (2021).** Features of various posterior cranial fossa tumors on Magnetic Resonance Imaging and their correlation with histopathological diagnosis. *American Journal of Health, Medicine and Nursing Practice*, 6(4): 40-88.
  - **Morani AC, Ramani NS, and Wesolowski JR. (2011).** Skull base, orbits, temporal bone, and cranial nerves: anatomy on MR imaging. *Magnetic Resonance Imaging Clinics*, 19(3), 439-456.
  - **Mulkens TH, Parizel PM, De Schepper AM, Van de Heyning PH, Forton GE, Martin JJ et al. (1993).** Kernspintomographie des Akustikusneurinoms (Schwannoms): Eine retrospektive Studie von 89 Tumoren. In *RöFo-Fortschritte auf dem Gebiet der Röntgenstrahlen und der bildgebenden Verfahren*, 158 (4): 362-367. © Georg Thieme Verlag Stuttgart· New York.
  - **O'Brien DF, Caird J, Kennedy M, Roberts GA, Marks JC, Allcutt DA et al. (2001).** Posterior fossa tumours in childhood: evaluation of presenting clinical features. *Irish medical journal*, 94(2): 52-53.
  - **Qiu SJ, Zhang XL. (2003).** MRI features of 13 cases of intracranial ependymoma. *Di 1 jun yi da xue*

xue bao= Academic Journal of the First Medical College of PLA, 23(11): 1224-1225.

- **Rodallec M, Colombat M, Krainik A, Kalamarides M, Redondo A, Feydy A. (2004).** Diffusion-weighted MR imaging and pathologic findings in adult cerebellar medulloblastoma. Journal of neuroradiology, 31(3), 234-237.
- **Zimmerman RA. (1996).** Neuroimaging of primary brainstem gliomas: diagnosis and course. Pediatric neurosurgery, 25(1), 45-53.